# A novel approach to predict acute radiation dermatitis in patients with head and neck cancer using a model based on Bayesian probability

濱田, 圭介



出版情報：Kyushu University, 2023, 博士（保健学）, 課程博士
バージョン：

Physica Medica 116 (2023) 103181

Contents lists available at ScienceDirect

Physica Medica

journal homepage: www.elsevier.com/locate/ejmp

# A novel approach to predict acute radiation dermatitis in patients with head and neck cancer using a model based on Bayesian probability

Keisuke Hamada [a,b,*], Toshioh Fujibuchi [c], Hiroyuki Arakawa [c], Yuichi Yokoyama [a], Naoki Yoshida [a], Hiroki Ohura [d], Naonobu Kunitake [e], Muneyuki Masuda [f], Takeo Honda [a], Satoru Tokuda [g], Makoto Sasaki [h]

[a] Department of Radiological Technology, National Hospital Organization Kyushu Cancer Center, 3-1-1, Notame, Minami-ku, Fukuoka City, Fukuoka 811-1395, Japan
[b] Department of Health Sciences, Graduate School of Medicine, Kyushu University, 3-1-1 Maidashi, Higashi-ku, Fukuoka 812-8582, Japan
[c] Department of Health Sciences, Faculty of Medical Sciences, Kyushu University, 3-1-1 Maidashi, Higashi-ku, Fukuoka 812-8582, Japan
[d] Department of Radiological Technology, National Hospital Organization Kyushu Medical Center, 1-8-1 Jigyohama, Chuo-ku, Fukuoka City, Fukuoka 810-8563, Japan
[e] Department of Radiation Oncology, National Hospital Organization Kyushu Cancer Center, 3-1-1, Notame, Minami-ku, Fukuoka City, Fukuoka 811-1395, Japan
[f] Department of Head and Neck Surgery, National Hospital Organization Kyushu Cancer Center, 3-1-1, Notame, Minami-ku, Fukuoka City, Fukuoka 811-1395, Japan
[g] Research Institute for Information Technology, Kyushu University, 6-1, Kasuga koen, Kasuga City, Fukuoka 816-8580, Japan
[h] College of Industrial Technology, Nihon University, 1-2-1 Izumi-cho, Narashino City, Chiba 275-8575, Japan

ARTICLE INFO

*Keywords:*
Bayesian probability
Acute radiation dermatitis
Probabilistic forecasting
Head and neck radiation therapy

ABSTRACT

*Purpose:* In this study, we aimed to establish a method for predicting the probability of each acute radiation dermatitis (ARD) grade during the head and neck Volumetric Modulated Arc Therapy (VMAT) radiotherapy planning phase based on Bayesian probability.
*Methods:* The skin dose volume >50 Gy ($V_{50}$), calculated using the treatment planning system, was used as a factor related to skin toxicity. The empirical distribution of each ARD grade relative to $V_{50}$ was obtained from the ARD grades of 119 patients (55, 50, and 14 patients with G1, G2, and G3, respectively) determined by head and neck cancer specialists. Using Bayes' theorem, the Bayesian probabilities of G1, G2, and G3 for each value of $V_{50}$ were calculated with an empirical distribution. Conversely, $V_{50}$ was obtained based on the Bayesian probabilities of G1, G2, and G3.
*Results:* The empirical distribution for each graded patient group demonstrated a normal distribution. The method predicted ARD grades with 92.4 % accuracy and provided a $V_{50}$ value for each grade. For example, using the graph, we could predict that $V_{50}$ should be $\leq$24.5 $cm^3$ to achieve G1 with 70 % probability.
*Conclusions:* The Bayesian probability-based ARD prediction method could predict the ARD grade at the treatment planning stage using limited patient diagnostic data that demonstrated a normal distribution. If the probability of an ARD grade is high, skin care can be initiated in advance. Furthermore, the $V_{50}$ value during treatment planning can provide radiation oncologists with data for strategies to reduce ARD.

## 1. Introduction

Radiation therapy for head and neck cancer preserves their function and shape and reduces impairments in speech, chewing, and swallowing functions [1–3]. Approximately 50 % of patients with head and neck cancer are treated with a combination of radiation therapy and chemoradiation [4–6]. Volumetric Modulated Arc Therapy (VMAT) for head and neck cancer delivers approximately 70 Gy of irradiation to the planned target volume of the tumor [7–9]. Severe acute radiation dermatitis (ARD) [10], such as erythema and desquamation, frequently occurs as an adverse effect, which interrupts the treatment schedules [11,12]. Therefore, the radiation oncologist can objectively consider

* Corresponding author at: Department of Radiological Technology, National Hospital Organization Kyushu Cancer Center, 3-1-1 Notame Minami-ku, Fukuoka City, Fukuoka 811-1395, Japan.
*E-mail addresses:* hamada.keisuke.we@mail.hosp.go.jp (K. Hamada), fujibuchi.toshioh.294@m.kyushu-u.ac.jp (T. Fujibuchi), arakawa.hiroyuki.306@m.kyushu-u.ac.jp (H. Arakawa), yokoyama.yuichi.jx@mail.hosp.go.jp (Y. Yokoyama), yoshida.naoki.hb@mail.hosp.go.jp (N. Yoshida), ooura.hiroki.uy@mail.hosp.go.jp (H. Ohura), kunitake.naonobu.nb@mail.hosp.go.jp (N. Kunitake), mmuneyuki@icloud.com (M. Masuda), honda.takeo.mn@mail.hosp.go.jp (T. Honda), s.tokuda.a96@m.kyushu-u.ac.jp (S. Tokuda), sasaki.makoto@nihon-u.ac.jp (M. Sasaki).

https://doi.org/10.1016/j.ejmp.2023.103181
Received 19 June 2023; Received in revised form 4 October 2023; Accepted 17 November 2023

treatment planning after obtaining probability prediction information according to factors, such as skin dose related to the onset and severity of ARD. Additionally, radiation oncologists can specifically communicate the need for skin care to medical staff based on ARD probabilistic predictive information, which is expected to have a preventive effect in reducing ARD.

Previous studies on ARD prediction for head and neck cancer radiotherapy have reported dose-volume histograms (DVHs) [13], correlations between skin dose and volume [13–18], and scoring [16]. All these reports discussed the thresholds for predicting and reducing ARD deterministically. Furthermore, ARD is reportedly dependent on factors that affect the skin surface dose, including chemotherapy [13–16], bolus effect [19,20], and beam angle [21]. We hypothesized that ARD predictions would be more clinical if they were discussed probabilistically rather than deterministically. Therefore, in this study, we focused on Bayesian probability as a method for probabilistically predicting ARD grades. Bayesian probability is effective for populations with unknown probability distributions, and it serves as a method for predicting uncertain events based on past experiences [22,23]. Even if the probability of ARD occurrence is unknown, a predictive model can be created using retrospective patient data with pre-determined ARD grades.

In this study, we aimed to use Bayesian probability to predict the probability of ARD during the treatment planning phase and also to obtain an indication of the V50 threshold at which severe ARD occurs. This new probabilistic prediction method may facilitate the management of ARD induced by head and neck VMAT.

## 2. Materials and methods

### 2.1. Clinical protocol

The treatment device used in this study was TrueBeam (Varian Medical Systems, Palo Alto, CA, USA), and the treatment planning system (TPS) used was Eclipse version 13.6 (Varian Medical Systems). Furthermore, the photon energy was 6 MV, the dose calculation grid size was set to 1.5 mm, and the computational algorithm used was Acuros XB. Similar to the Monte Carlo simulation, Acuros XB assigns physical densities to six substances, namely, air, lung, fat, skeletal muscle, cartilage, and bone, based on computed tomography numbers. These six substances were also used to calculate the mass collision stopping power when calculating the dose delivery from the electron fluence [24]. The thermoplastic mask (CIVCO Radiotherapy, Orange City, IA, USA) had a thickness and hole diameter of 1.6 mm and 4 mm, respectively. This study was approved by the ethics committee of Kyushu Cancer Center (2022–30) and was conducted according to the Declaration of Helsinki. All participants provided written informed consent before the start of the study.

Target volumes were delineated as follows: the gross tumor volume (GTV) included the gross extent of the primary disease and involved lymph node metastases, considering clinical and radiological findings; clinical target volume (CTV) was defined as the area of GTV plus a 5-mm margin, considering anatomical and clinical oncological features. The planning target volume (PTV) was defined by adding a 5-mm margin to the CTV. Notably, 2 mm of PTV was excluded from the skin surface to avoid overdosing the skin under the assumption that the CTV dose would not be sacrificed. In selected cases (i.e., superficial GTV and skin infiltration), a smaller (1 or 2 mm) or no margin was applied. In accordance with our institutional policy, a bolus was never applied. Tumor staging was performed using the malignant tumor criteria of the Union for International Cancer Control (8th edition) [25].

This retrospective study included patients with head and neck cancer who underwent VMAT and received concurrent chemoradiation at the Kyushu Cancer Center. All patients were treated in five fractions per week, with 2.0 Gy/fraction, and a total of 35 fractions of 70 Gy per patient. A two-step method of VMAT was used. The first plan involved irradiating the primary, nodal, and prophylactic CTVs with 40 Gy. Subsequently, the primary and nodal CTVs were irradiated with 30 Gy up to 70 Gy. All patients were prophylactically irradiated in bilateral lymph node areas, and the median overall treatment time was 48 days (range, 47–49 days). The rotation angle of VMAT is 360° (full arc VMAT). The angle of rotation of VMAT affects the accuracy of TPS calculations, with Akino et al. reporting that partial arc VMAT does not provide accurate skin dose calculations [26] and Lowther et al. reporting that full arc VMAT skin dose calculations are accurate [27]. The 119 patients enrolled in this study received radiotherapy with full arc VMAT. 3-dimensional conformal radiation therapy (3DCRT) was not included in this study because the dose administered was 60 Gy and the dose distribution was different.

### 2.2. Patient characteristics

This study included VMAT patients who received head and neck radiation therapy from July 1, 2019, to July 31, 2022. Of the 146 patients who underwent VMAT, 119 (106 male and 13 female) were finally enrolled in this study after excluding 14 whose treatment plan was changed to surgery and 13 who discontinued radiotherapy.

The median age of the patients was 65 years (range, 38–91 years; male 65.7±10.4 years and female 57.9±13.7 years). The primary tumor sites were the epiglottis (n = 13; 11 %), mesopharynx (n = 42; 35 %), hypopharynx (n = 36; 30 %), larynx (n = 12; 10 %), tongue (n = 6; 5 %), tonsils (n = 6; 5 %), floor of the mouth (n = 2; 2 %), hard palate (n = 1; 1 %), and subauricular glands (n = 1; 1 %). All patients underwent concurrent chemoradiotherapy (100 %), and the drugs administered were as follows: cisplatin (n = 103; 86 %), nedaplatin (n = 12; 10 %), fluorouracil (n = 2; 2 %), and carboplatin (n = 2; 2 %). Classification based on tumor histology revealed 113 (95 %) squamous cell carcinomas and 6 (5 %) adenocarcinomas. Moreover, 26 (21.5 %), 47 (39.5 %), 31 (26.1 %), and 15 (12.6 %) patients were diagnosed with stages I, II, III, and IV disease, respectively. Patient characteristics are presented in Table 1.

The skin ring structure was semi-automatically created by subtracting 2 mm from the external patient surface. The skin surface dose obtained using TPS was converted to DVH parameters to obtain dose information.

### 2.3. Evaluation of ARD

The retrospective data for skin dose volume ($V_{50}$) were obtained from TPS, and the ARD grade was diagnosed by the head and neck cancer physician according to the Common Terminology Criteria for Adverse Events (CTCAE) v5.0 [10].

All patient ARD evaluations were performed within 3 days of the end of radiotherapy. The highest toxicity grade was used as a reference. The CTCAE for dermatitis was defined as follows: grade 1, faint erythema or dry desquamation; grade 2, moderate to brisk erythema, patchy moist desquamation (mostly confined to skin folds and creases), and moderate edema; grade 3, moist desquamation in areas other than skin folds and creases, and bleeding induced by minor trauma or abrasion; and grade 4, life-threatening skin necrosis or ulceration of the full-thickness dermis, spontaneous bleeding, and a need for skin grafts. The predicted grades were as follows: G1, 55 (46 %) patients; G2, 50 (42 %) patients; and G3, 14 (12 %) patients (Table 1).

The Bayesian probability of ARD grade was defined according to the value of $V_{50}$. In previous studies, $V_{60}$ [14,15] were given as indicators, and doses of 50–60 Gy were within the range of radiation dermatitis prediction indicators [14]. No data above $V_{60}$ were available for this study; therefore, the highest $V_{50}$ was selected. In this study, V50 was considered a factor related to skin toxicity and was used as the variable of interest X in the Bayesian probability. Based on Bayes' theorem, the Bayesian probabilities of G1, G2, and G3 were determined according to the $V_{50}$ values. The grade with the highest probability was considered the predicted ARD grade, and it was compared with that diagnosed by a head and neck cancer specialist. $V_{50}$ was also obtained based on the

**Table 1**
Summary of patient characteristics.

| Age (years) 38–91 (median 65) | | | | |
|---|---|---|---|---|
| Patient characteristics | Number (%) of patients | | | |
| Sex | | | | |
| Male | 106 (89 %) | | | |
| Female | 13 (11 %) | | | |
| Age (years) | | | | |
| Male | 65.7±10.4 | | | |
| Female | 57.9±13.7 | | | |
| Tumor site | | | | |
| Epiglottis | 13 (11 %) | | | |
| Mesopharynx | 42 (35 %) | | | |
| Hypopharynx | 36 (30 %) | | | |
| Larynx | 12 (10 %) | | | |
| Tongue | 6 (5 %) | | | |
| Tonsils | 6 (5 %) | | | |
| Floor of mouth | 2 (2 %) | | | |
| Hard palate | 1 (1 %) | | | |
| Subauricular glands | 1 (1 %) | | | |
| Histology | | | | |
| Squamous cell carcinoma | 113 (95 %) | | | |
| Adenocarcinoma | 6 (5 %) | | | |
| Neoadjuvant | | | | |
| (+) | 0 (0 %) | | | |
| (-) | 119 (100 %) | | | |
| Concurrent | | | | |
| (+) | 119 (100 %) | | | |
| (-) | 0 (0 %) | | | |
| Types of anticancer drugs | | | | |
| Cisplatin | 103 (86 %) | | | |
| Nedaplatin | 12 (10 %) | | | |
| Fluorouracil | 2 (2 %) | | | |
| Carboplatin | 2 (2 %) | | | |
| Acute toxicity grade | | | | |
| G1/G2/G3 | 55/50/14 | | | |
| Smoking | | | | |
| Never/former | 30 (25 %) | | | |
| Current | 89 (75 %) | | | |
| Interruption of radiation therapy | | | | |
| Temporary suspension | 0 (0 %) | | | |
| Accomplished | 119 (100 %) | | | |
| Surgical | | | | |
| Yes | 0 (0 %) | | | |
| No | 119 (100 %) | | | |
| VMAT | | | | |
| Full arc | 119 (100 %) | | | |
| Partial arc | 0 (0 %) | | | |
| TNM stage | N0 | N1 | N2 | N3 |
| T0–1 | 4 (3.4 %) | 12 (10.1 %) | 6 (5.0 %) | 4 (3.4 %) |
| T2 | 11 (9.2 %) | 20 (16.8 %) | 15 (12.6 %) | 1 (0.8 %) |
| T3 | 9 (7.6 %) | 9 (7.6 %) | 8 (6.7 %) | 5 (4.2 %) |
| T4 | 0 (0.0 %) | 7 (5.9 %) | 5 (4.2 %) | 3 (2.5 %) |

VMAT, Volumetric Modulated Arc Therapy; G1, Grade 1; G2, Grade 2; G3, Grade 3.

probabilities of G1, G2, and G3.

Statistical analyses were performed using EZR (Easy R) version 1.51 (Saitama Medical Center, Jichi Medical University, Saitama, Japan), which is a graphical user interface for R (The R Foundation for Statistical Computing, Vienna, Austria) [28]. The Shapiro–Wilk test was used to evaluate the normality of the irradiation volume distribution for each ARD grade. A p-value of 0.05 or greater for a sample was considered a normal distribution.

### 2.4. Bayesian probability of ARD

Bayes' theorem is a formula for determining conditional probability. Given a set of conditions, it is possible to calculate how these conditions change the probability of other events [29,30].

The Bayesian probability is evaluated using the following equation:

$$P(G_i|X) = \frac{P(\mathrm{X}|G_i)P(G_i)}{\sum_{i=1}^{n} P(\mathrm{X}|G_i)P(G_i)} \quad (1)$$

*Gi*: ($i = 1,2,3$),

where the left-hand side $P(Gi|X)$ of Eq. (1) is the probability that the ARD grade (*Gi*) is predicted when X, the value of $V_{50}$, is obtained. The numerator $P(X|Gi)$ on the right-hand side is the probability of X when a certain ARD grade (*Gi*) is obtained, and $P(Gi)$ is the frequency distribution for each ARD grade. The denominator $\sum_{i=1}^{n} P(\mathrm{X}|G_i)P(G_i)$ on the right side is the normalization factor such that the sum of all probabilities on the right side is 1. $P(X|Gi)$ was modeled as a normal distribution defined based on the sample mean and standard deviation of $V_{50}$. When following a normal distribution, Bayesian probability has the advantage that accurate probabilistic predictions are possible even with small numbers of patients [22,23,31,32]. Here, the probability of each *Gi* is represented as $P(Gi)$, $i = 1,2,3$.

Fig. 1 shows the process by which the Bayesian probabilities of ARD grades relative to $V_{50}$ were obtained and the workflow for predicting the grade probability from the $V_{50}$ of a new patient.

The Bayesian probabilities used the skin dose volume ($V_{50}$) of the 119 patients calculated using the TPS, as described in Fig. 1(i), and the *Gi* of the 119 patients diagnosed by a head and neck cancer specialist, as described in Fig. 1(ii). Furthermore, $V_{50}$ was used as a random variable and factors related to skin toxicity.

First, we determined the empirical distribution of *Gi* corresponding to $V_{50}$, as described in Fig. 1(iii). The empirical distribution was a normal distribution defined based on the sample mean and sample standard deviation of *Gi* (Fig. 1(ii)) corresponding to $V_{50}$ (Fig. 1(i)). Second, we calculated the Bayesian probabilities of radiation dermatitis grades relative to $V_{50}$, as described in Fig. 1(iv). The empirical distribution demonstrated in Fig. 1(iii) was multiplied by the frequency distribution described in Fig. 1(ii). The frequency distribution was based on the ARD grade for 119 patients diagnosed by a head and neck cancer specialist, with 55, 50, and 14 patients in G1, G2, and G3, respectively. Finally, we determined the probability of each ARD grade with respect to $V_{50}$.

When the $V_{50}$ of a new patient is applied to the Bayesian probabilities for ARD grades, the Bayesian probabilities of Gi for $V_{50}$ can predict the ARD grade for a patient in the planning phase of the treatment probabilistically.

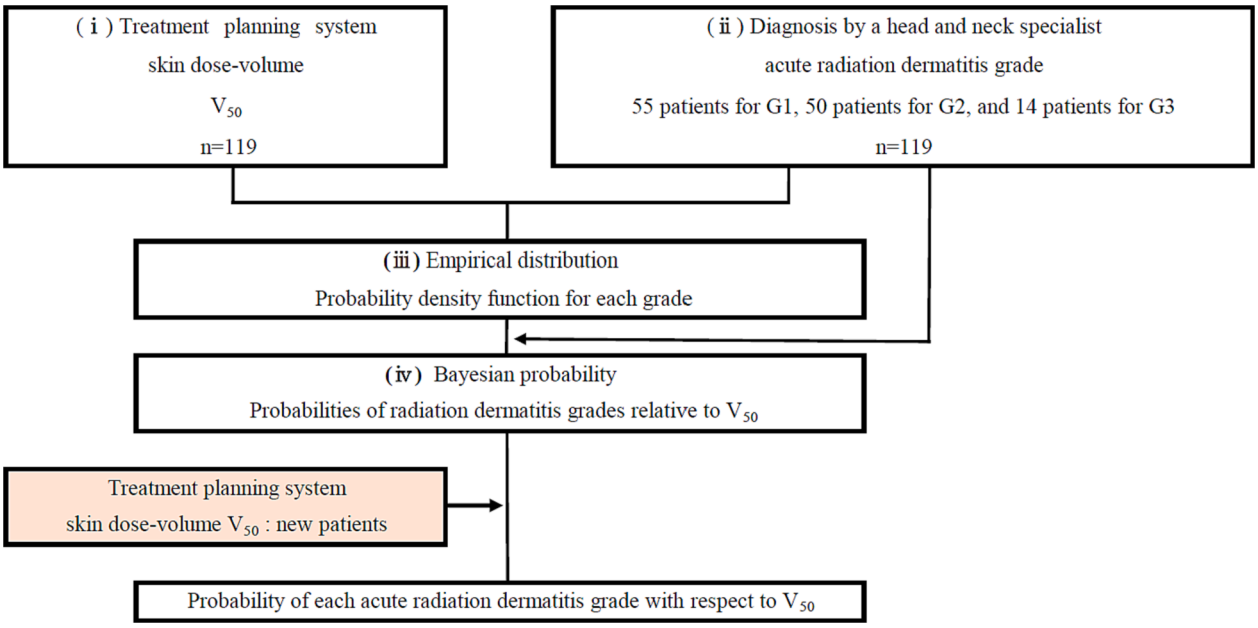


**Fig. 1.** Workflow for obtaining Bayesian probability of ARD grade for $V_{50}$. Fig. 1(i) shows the skin dose volume ($V_{50}$) for 119 patients calculated using the treatment planning system. Fig. 1(ii) shows the ARD grades (G1, G2, and G3) of the 119 patients diagnosed by a head and neck cancer specialist. Fig. 1(iii) shows the empirical distributions of G1, G2, and G3, corresponding to $V_{50}$. Fig. 1(iv) shows the Bayesian probability of the radiation dermatitis grade relative to $V_{50}$. ARD, acute radiation dermatitis.

### *2.5. Examples of evaluating ARD grade predictions and setting thresholds using a model based on Bayesian probability*

The predicted grade from Bayesian probability was determined using the grade with the highest probability of occurrence. The agreement between the predicted ARD grade and the ARD grade diagnosed by the head and neck cancer specialist was assessed based on the number of patients with each grade who exhibited clinical symptoms and the percentage of those whose predicted grades matched.

$V_{50}$ was determined from the inverse function of the Bayesian probability of the radiation dermatitis grade as a function of $V_{50}$ (Fig. 2). Using the Bayesian probabilities of radiation dermatitis grades as a function of $V_{50}$, the probability of each grade was selected based on the vertical axis in Fig. 2, and $V_{50}$ for that grade was determined.

Since G2 is not a monotonically increasing probability, two $V_{50}$ values were obtained for the probabilities, except for the peak

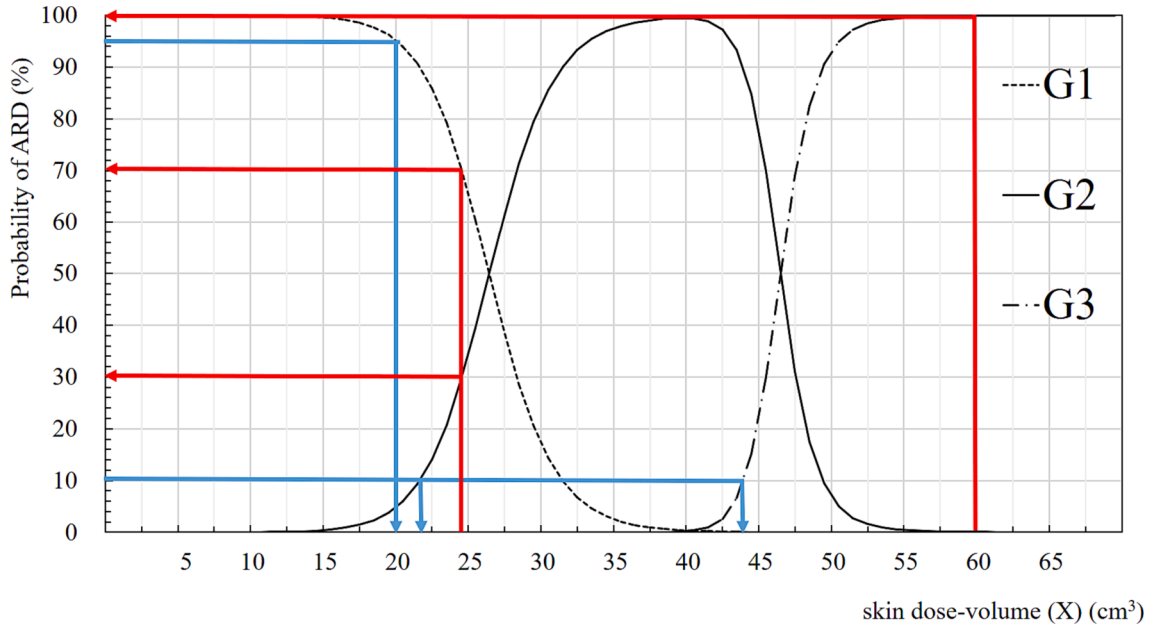


**Fig. 2.** Bayesian probabilities of ARD grades relative to $V_{50}$. The red line represents a probabilistic prediction for ARD. For example, a new patient with a $V_{50}$ value of 24.5 $cm^3$ would be predicted to have a 70 % and 30 % probability of G1 and G2, respectively. If the $V_{50}$ value of the new patient is 60.0 $cm^3$, the probability of G3 can be predicted to be 100 %. The blue line represents a treatment plan optimization. When optimizing the probability of G1 to 95 %, the skin dose volume should be $<$20.0 $cm^3$. When optimizing the probabilities of G2 and G3 to 10 %, the skin dose volumes should be $<$22.0 $cm^3$ and $<$44.5 $cm^3$, respectively. ARD, acute radiation dermatitis; G1, Grade 1; G2, Grade 2; G3, Grade 3. (For interpretation of the references to colour in this figure legend, the reader is referred to the web version of this article.)

probability. In this case, a low $V_{50}$ value was selected because a high $V_{50}$ value is meaningless with respect to reducing skin damage. For example, we determined the $V_{50}$ value at which the probabilities of G1, G2, and G3 were >95 %, 10 %, and 10 %, respectively.

### 2.6. Factors related to skin toxicity

Factors related to skin toxicity considered in previous studies include patient [13–18,33–52] (Supplementary Table 1) and device factors [13,16,20,33,45,47,51,53–69] (Supplementary Table 2). The association with ARD is ambiguous; some factors can be inferred to be associated with ARD from previous studies. Factors on which there is a disagreement also exist. Therefore, we have compiled factors related to skin toxicity from previous studies in the supplemental material to identify those associated with ARD (Supplementary Tables 1 and 2).

## 3. Results

### 3.1. Probabilistic model of skin dose volume

Fig. 3 shows the probability density function and histogram of the number of patients. $P(X|G1)$ is the probability density function of X corresponding to a G1 patient, $P(X|G2)$ is the probability distribution function of X corresponding to a G2 patient, and $P(X|G3)$ is the probability density function of X corresponding to a G3 patient.

P-values (using the Shapiro–Wilk test) for *Gi* were 0.0952 ($p > 0.05$), 0.2383 ($p > 0.05$), and 0.1541 ($p > 0.05$) for G1, G2, and G3, respectively. Each probability density function shown in Fig. 3 is normally distributed.

### 3.2. Bayesian probability of ARD

Fig. 2 shows the probability of the ARD grade versus $V_{50}$. The $V_{50}$ value of a new patient was obtained from TPS, and the ARD grade was predicted using this Bayesian probability.

Fig. 2 shows the relationship between ARD grade probability and $V_{50}$. The horizontal and vertical axes represent the skin dose volume and probability of ARD, respectively. The $V_{50}$ values of new patients were obtained from TPS calculations, and a probabilistic ARD prediction model based on Bayesian probability was used. The red line represents a probabilistic prediction for ARD. For example, if the skin dose volume of $V_{50}$ calculated using TPS is 24.5 $cm^3$, the probability of G1 can be predicted to be 70 % based on the intersection of 24.5 $cm^3$ and the dotted line G1 on the horizontal axis. Furthermore, the probability of G2 can be predicted to be 30 % based on the intersection of the solid line with G2. Moreover, if the $V_{50}$ value of the new patient is 60.0 $cm^3$, the probability of G3 can be predicted to be 100 %. Therefore, a Bayesian probability-based ARD prediction model can be used to predict the ARD grade of new patients.

### 3.3. Examples of evaluating ARD grade predictions and setting thresholds using a model based on Bayesian probability

For G1, 51 of the 55 participants agreed, with a 92.7 % agreement rate. For G2, 46 of the 50 participants agreed, with a 92.0 % agreement rate. For G3, 13 of the 14 participants agreed, with a 92.9 % agreement rate. Overall, 110 of the 119 patients agreed, with a 92.4 % agreement rate.

Fig. 2 shows an example of treatment plan optimization using a probabilistic ARD prediction model based on Bayesian probability. For example, when planning a treatment with a 95 % probability of G1 occurring, the skin dose volume can be predicted to be ≤20.0 $cm^3$ from the point where the 95 % of the vertical axis of the prediction model and the dotted G1 intersect. Similarly, when planning a treatment plan with a 10 % probability of G2 and G3 occurring, the skin dose volume can be predicted to be ≤22.0 $cm^3$ from the point where G2 intersects the solid line, and the skin dose volume should be ≤44.5 $cm^3$ from the point where G3 intersects the dashed line. Therefore, a probabilistic predictive model can be used to predict ARD and optimize treatment planning.

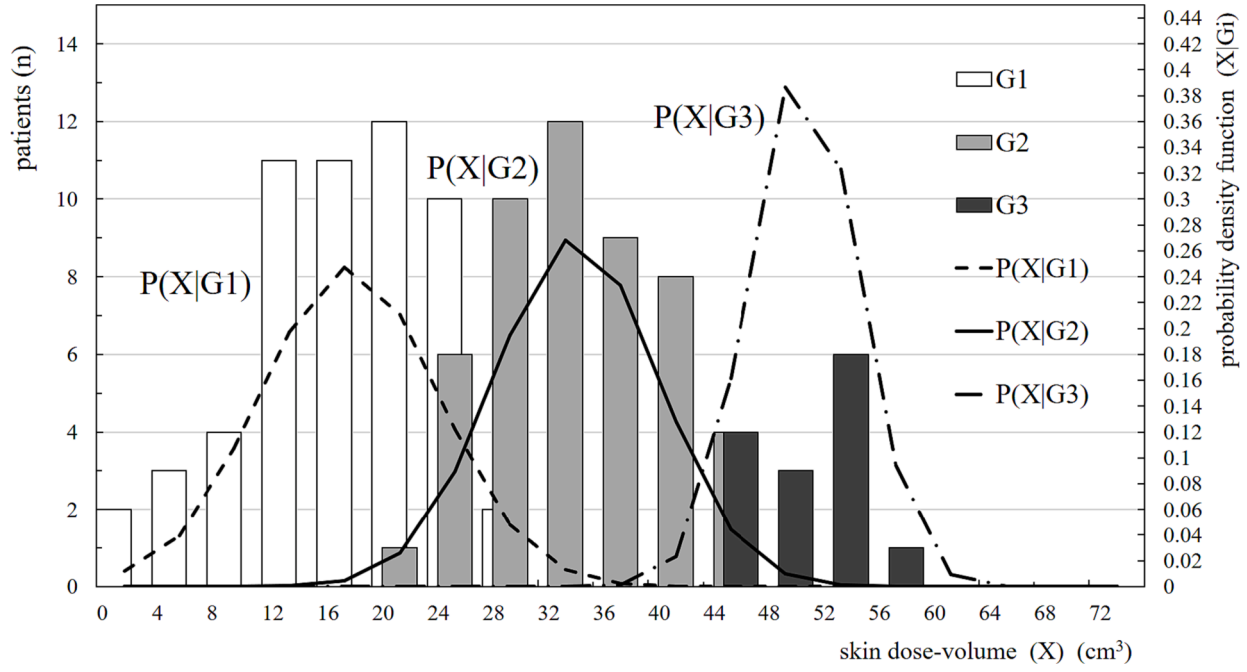


**Fig. 3.** Patients distribution and skin dose-volume for each grade. The abscissa represents the skin dose volume of $V_{50}$, and the ordinate represents the number of patients and probability density function. The dotted line $P(X|G1)$, solid line $P(X|G2)$, and dashed line $P(X|G3)$ are the probability density functions for G1, G2, and G3, respectively. The white, gray, and dark gray bar charts indicate the number of patients with G1, G2, and G3, respectively. G1, Grade 1; G2, Grade 2; G3, Grade 3.

## 4. Discussion

### 4.1. Probabilistic forecasting

This study proposes a method for predicting ARD based on Bayesian probability. The proposed method predicts ARD grade probabilistically based on previous ARD grades as diagnosed by head and neck physicians and the corresponding $V_{50}$ data, even if the probability of the ARD grade was unknown at the treatment planning stage. To the best of our knowledge, this is the first report about a method for probabilistically predicting ARD.

Previous studies have provided various ARD forecasting indicators. Table 2 lists their evaluation methods and characteristics. It summarizes the total number of patients, prediction indicators, number (n) and percentage (%) of patients used for prediction, ARD grade for all prediction methods, thresholds, and chemotherapy information. A common feature of previous studies [13–15] is that they set the thresholds deterministically. However, our proposed prediction method could also predict each grade probabilistically.

Notably, the results shown in Fig. 3 indicate that G1/G2 and G2/G3 overlap. Although the $V_{50}$ values calculated using TPS are the same, the ARD grade results will differ due to the influence of patient factors (Supplementary Table 1). Existing methods do not consider this overlap of data and describe it deterministically. By contrast, the method used in this study can show these data overlap probabilistically.

### 4.2. Statistics required for prediction

Previous studies have reported varying thresholds for ARD reduction (Table 2) since ARD is influenced by device-related factors (Supplementary Materials) [16]. We believe that the optimal index varies across facilities, depending on the treatment and device. We assumed that the predictive indicators are most accurate when created facility-by-facility. However, if predictive indicators are developed for each facility, the sample size will be smaller, and the statistical power will inevitably be reduced. Furthermore, in previous studies [13–15], the prediction indicators were grouped into “severe/moderate (G3/G2),” “severe (G3/G4),” and “mild (G1/G2)” for statistical analysis. The reason for grouping each grade was to ensure a sufficient number of cases for statistical analysis, as previous studies have cited limited cases in the predictive index as limitations to their investigation [13–15] (Table 2). Generally, ARDs are classified according to clinical symptoms from grades 1 to 4, as described in Section 2.3 [10]. Therefore, it is ideal to present forecasting indicators based on grades. This study had the advantage of making effective predictions despite having limited data. A sample size range of 7–2000 is recommended for the Shapiro–Wilk test to determine the normal distribution [70]. The minimum sample size is the number of data items that would be normally distributed using the Shapiro–Wilk test. This minimum sample size cannot be asserted as it is affected by the factors related to skin toxicity and the facility’s patient data. If the sample size is small and not normally distributed, data can be added subsequently for analysis [29,30]. In this study, the number of patients followed a normal distribution, which enabled us to present the probabilities for each grade.

### 4.3. Application to the optimization of treatment planning

Using the method proposed in this study, the ARD grade could be predicted probabilistically from the $V_{50}$ values, and the $V_{50}$ values could also be determined from the probability of each grade. Furthermore, $V_{50}$ values were useful for optimizing treatment planning. If ARD can be predicted from $V_{50}$ values during the planning phase of the treatment, radiation oncologists can quantitatively optimize the dose according to the risk of ARD in individual patients. In this case, the risk of a reduced target dose should be considered [27]. The development of individually optimized treatment plans aims to reduce the severity of ARD [13]. Therefore, indicators that probabilistically predict the ARD grade, rather than using conventional deterministic evaluations, can aid radiation oncologists in treatment planning.

The ARD evaluation in this study was performed within 3 days after the end of radiotherapy. ARD reaches peak symptoms 1–2 weeks after radiotherapy completion [71]. Therefore, the ARD assessment was conducted before the peak of ARD symptoms was reached, which may have underestimated the predicted results. A more accurate prediction

**Table 2**
Comparison of predictive indicators between previous studies and this study.

| Authors | Total number of patients | Prediction indicators | Number (%) of patients used for prediction | ARD grade of all patients | Prediction method | Threshold | Fractionation | Chemotherapy information |
|---|---|---|---|---|---|---|---|---|
| Mori et al. [13] | 70 | G2/G3 | G2/G3 n = 43 (61.4 %) | G0/G1 n = 27 (38.6 %), G2 = 30 (42.9 %), G3 n = 13 (18.6 %) | Deterministic | G2/G3 prediction: $V_{56}$ 7.7 cc<br>G3 prediction: $V_{60}$ 3 cc | 54/66 Gy: 30 Fr.<br>69 Gy: 30 Fr. | without cetuximab |
| Bonomo et al. [14] | 90 | G3/G4 | G3/G4 n = 37 (41.1 %) | G1/G2 n = 53 (58.9 %) G3/G4 n = 37 (41.1 %) | Deterministic | G3/G4 prediction: $V_{60}$ 5.8 cc<br>G1/G2 prediction: $V_{50}$ 19.9 cc | 66–70.5 Gy: 30–35 Fr. | cetuximab and cisplatin cohort |
| Studer et al. [15] | 99 | G3/G4 | G3/G4 n = 34 (34.3 %) | G0/G1/G2 n = 65 (65.7 %), G3/G4 n = 34 (34.3 %) | Deterministic | G3/G4 prediction: $V_{60}$ 30 cc | 70 Gy: 30 Fr.<br>69.6 Gy: 30 Fr. | cetuximab cohort |
| | 99 | G3/G4 | G3/G4 n = 3 (3.0 %) | G0/G1/G2 n = 96 (97 %), G3/G4 n = 3 (3 %) | | G3/G4 prediction: $V_{50}$ 15 cc | | cisplatin cohort |
| Current study | 119 | G1, G2, and G3 | G1 n = 55 (46.2 %), G2 n = 50 (42.0 %), G3 n = 14 (11.8 %) | G1 n = 55 (46.2 %), G2 n = 50 (42.0 %), G3 n = 14 (11.8 %) | Probabilistic | $V_{50}$ 25 $cm^3$<br>80 % probability of G1<br>20 % probability of G2 | 70 Gy: 35 Fr. | without cetuximab |

ARD, acute radiation dermatitis; G1, Grade 1; G2, Grade 2; G3, Grade 3; G4, Grade 4; $V_{56}$, volume greater than 56 Gy; $V_{60}$, volume greater than 60 Gy; $V_{56}$, volume greater than 56 Gy; $V_{50}$, volume greater than 50 Fr.; fractionation.

may be possible if the ARD evaluation is performed 1–2 weeks after radiotherapy completion. In our hospital, patients were discharged within 3 days of radiotherapy completion, which was a limitation for the ARD evaluation.

### 4.4. Limitation

Factors affecting skin toxicity are summarized in Supplementary Tables 1 and 2 for individual patient and device factors, respectively. In this study, factors related to skin toxicity were defined as $V_{50}$; however, more appropriate factors affecting skin toxicity may be obtained depending on the treatment method and equipment used at each facility. Therefore, we cannot assert that $V_{50}$ is the best factor related to skin toxicity. In some facilities, $V_{60}$ may be a better factor associated with skin toxicity. As a factor related to skin toxicity, doses lower than $V_{50}$ are not predictive indicators of ARD [13,14]. ARD has been reported to be caused by various combinations of factors other than skin dose volume, which can increase the severity of ARD [16]. Factors contributing to ARD can be categorized into those for the individual patient and the equipment at each facility. Individual patient factors include chemotherapy drugs, genetic information, patient overall status, nutritional state, weight loss, and body mass index (Supplementary Table 1). Device factors include the characteristics of the treatment device in possession, the characteristics of the irradiation technique, the thickness of the thermoplastic mask and bolus, and the total dose (Supplementary Table 2). The number and combination of these factors will vary for individual patients and institutions. Although skin DVH is an important indicator of ARD prediction, previous studies [13–15] have not identified an optimal skin dose volume. We have summarized the factors affecting skin toxicity in Supplementary Tables 1 and 2. Overall, various factors exist that influence skin toxicity, including those of individual patients and devices. Therefore, to improve the prediction accuracy, it is advisable to create a model that is appropriate for your facility's situation, referring to the factors shown in Supplementary Tables 1 and 2. Additionally, it is necessary to obtain large amounts of data in multicenter studies to create models that include various factors.

## 5. Conclusion

In this study, we proposed a method for predicting ARD grade based on Bayesian probability. Based on the correspondence between $V_{50}$ values from the treatment plan and the ARD grade diagnosed by the head and neck cancer specialist, the correspondence between the Bayesian probability of the ARD grade and $V_{50}$ values was determined. We presented predicting indices for each ARD grade because Bayesian probability enables valid forecasts in normally distributed frequencies, even with limited statistical data. The obtained correspondence could probabilistically predict the ARD grade of a new patient. Additionally, the probability of each grade provides $V_{50}$ values, which is an indicator for optimizing the treatment plan. Notably, understanding the factors that induce ARD improves the accuracy of the prediction. This novel Bayesian probability-based ARD prediction method will be an innovative tool for future ARD prediction as it will help manage ARD induced by head and neck VMAT and is a method that can probabilistically predict ARD in other populations and other hospitals.

## Declaration of Competing Interest

The authors declare that they have no known competing financial interests or personal relationships that could have appeared to influence the work reported in this paper.

## Funding

This study was funded internally by Kyushu University.

## Appendix A. Supplementary data

Supplementary data to this article can be found online at https://doi.org/10.1016/j.ejmp.2023.103181.

## References

[1] Bozec A, Culié D, Poissonnet G, Dassonville O. Current role of total laryngectomy in the era of organ preservation. Cancers 2020;12:584. https://doi.org/10.3390/cancers12030584.
[2] Anderson G, Ebadi M, Vo K, Novak J, Govindarajan A, Amini A. An updated review on head and neck cancer treatment with radiation therapy. Cancers 2021;13:4912. https://doi.org/10.3390/cancers13194912.
[3] Gamez ME, Blakaj A, Zoller W, Bonomi M, Blakaj DM. Emerging concepts and novel strategies in radiation therapy for laryngeal cancer management. Cancers 2020;12:1651. https://doi.org/10.3390/cancers12061651.
[4] Kaidar-Person O, Gil Z, Billan S. Precision medicine in head and neck cancer. Drug Resist Updat 2018;40:13–6. https://doi.org/10.1016/j.drup.2018.09.001.
[5] Lalla RV, Brennan MT, Gordon SM, Sonis ST, Rosenthal DI, Keefe DM. Oral mucositis due to high-dose chemotherapy and/or head and neck radiation therapy. J Natl Cancer Inst Monogr 2019; 2019::lgz011. https://doi.org/10.1093/jncimonographs/lgz011.
[6] Brook I. Late side effects of radiation treatment for head and neck cancer. Radiat Oncol J 2020;38:84–92. https://doi.org/10.3857/roj.2020.00213.
[7] Zahid MU, Mohamed ASR, Caudell JJ, Harrison LB, Fuller CD, Moros EG, et al. Dynamics-adapted radiotherapy dose (DARD) for head and neck cancer radiotherapy dose personalization. J Pers Med 2021;11:1124. https://doi.org/10.3390/jpm11111124.
[8] Zahid MU, Mohsin N, Mohamed ASR, Caudell JJ, Harrison LB, Fuller CD, et al. Forecasting individual patient response to radiation therapy in head and neck cancer with a dynamic carrying capacity model. Int J Radiat Oncol Biol Phys 2021;111:693–704. https://doi.org/10.1016/j.ijrobp.2021.05.132.
[9] Bourhis J, Tao Y, Sun X, Sire C, Martin L, Liem X, et al. LBA35 Avelumab-cetuximab-radiotherapy versus standards of care in patients with locally advanced squamous cell carcinoma of head and neck (LA-SCCHN): randomized phase III GORTEC-REACH trial. Ann Oncol 2021;32:S1310. https://doi.org/10.1016/j.annonc.2021.08.2112.
[10] Common terminology criteria for adverse events (CTCAE). version 5.0. [accessed 15 January 2019].
[11] Ferreira EB, Ciol MA, de Meneses AG, Bontempo PSM, Hoffman JM, Reis PEDD. Chamomile gel versus urea cream to prevent acute radiation dermatitis in head and neck cancer patients: results from a preliminary clinical trial. Integr Cancer Ther 2020;19. https://doi.org/10.1177/1534735420962174.
[12] Guimond E, Tsai CJ, Hosni A, O'Kane G, Yang J, Barry A. Safety and tolerability of metastasis-directed radiation therapy in the era of evolving systemic, immune, and targeted therapies. Adv Radiat Oncol 2022;7:101022. https://doi.org/10.1016/j.adro.2022.101022.
[13] Mori M, Cattaneo GM, Dell'Oca I, Foti S, Calandrino R, Di Muzio NG, et al. Skin DVHs predict cutaneous toxicity in head and neck cancer patients treated with tomotherapy. Phys Med 2019;59:133–41. https://doi.org/10.1016/j.ejmp.2019.02.015.
[14] Bonomo P, Talamonti C, Desideri I, Marrazzo L, Pezzulla D, Rampini A, et al. Analysis of skin dose distribution for the prediction of severe radiation dermatitis in head and neck squamous cell carcinoma patients treated with concurrent chemo-radiotherapy. Head Neck 2020;42:244–53. https://doi.org/10.1002/hed.25997.
[15] Studer G, Brown M, Salgueiro EB, Schmückle H, Romancuk N, Winkler G, et al. Grade 3/4 dermatitis in head and neck cancer patients treated with concurrent cetuximab and IMRT. Int J Radiat Oncol Biol Phys 2011;81:110–7. https://doi.org/10.1016/j.ijrobp.2010.05.018.
[16] Kawamura M, Yoshimura M, Asada H, Nakamura M, Matsuo Y, Mizowaki T. A scoring system predicting acute radiation dermatitis in patients with head and neck cancer treated with intensity-modulated radiotherapy. Radiat Oncol 2019;14:14. https://doi.org/10.1186/s13014-019-1215-2.
[17] Giro C, Berger B, Bölke E, Ciernik IF, Duprez F, Locati L, et al. High rate of severe radiation dermatitis during radiation therapy with concurrent cetuximab in head and neck cancer: results of a survey in EORTC institutes. Radiother Oncol 2009;90:166–71. https://doi.org/10.1016/j.radonc.2008.09.007.
[18] Bernier J, Bonner J, Vermorken JB, Bensadoun RJ, Dummer R, Giralt J, et al. Consensus guidelines for the management of radiation dermatitis and coexisting acne-like rash in patients receiving radiotherapy plus EGFR inhibitors for the treatment of squamous cell carcinoma of the head and neck. Ann Oncol 2008;19:142–9. https://doi.org/10.1093/annonc/mdm400.
[19] Wang L, Cmelak AJ, Ding GX. A simple technique to improve calculated skin dose accuracy in a commercial treatment planning system. J Appl Clin Med Phys 2018;19:191–7. https://doi.org/10.1002/acm2.12275.
[20] Kesen ND, Koksal C. Investigation of surface and buildup region doses for 6 MV high energy photon beams in the presence of a thermoplastic mask. Int J Radiat Res 2020;18:623–31. https://doi.org/10.52547/ijrr.18.4.623.
[21] O'Grady F, Barsky AR, Anamalayil S, Freedman GM, Kennedy C, Cai B, et al. Increase in superficial dose in whole-breast irradiation with Halcyon straight-through linac compared with traditional C-arm linac with flattening filter: in vivo dosimetry and planning study. Adv Radiat Oncol 2020;5:120–6. https://doi.org/10.1016/j.adro.2019.07.011.

[22] van de Schoot R, Depaoli S, King R, Kramer B, Märtens K, Tadesse MG, et al. Bayesian statistics and modelling. Nat Rev Methods Primers 2021;1:1–26. https://doi.org/10.1038/s43586-020-00001-2.

[23] Wu J, Chen XY, Zhang H, Xiong LD, Lei H, Deng SH. Hyperparameter optimization for machine learning models based on Bayesian optimization. J Electron Sci Technol 2019;17:26–40. https://doi.org/10.11989/JEST.1674-862X.80904120.

[24] Yousif YAM, Zifodya J. Dosimetric evaluation of a treatment planning system using the AAPM Medical Physics Practice Guideline 5.a (MPPG 5.a) validation tests. Phys Eng Sci Med 2022;45:1341–53. https://doi.org/10.1007/s13246-022-01194-4.

[25] Brierley JD, Gospodarowicz MK, Wittekind C, editors. TNM classification of malignant tumours. John Wiley & Sons; 2016.

[26] Akino Y, Das IJ, Bartlett GK, Zhang H, Thompson E, Zook JE. Evaluation of superficial dosimetry between treatment planning system and measurement for several breast cancer treatment techniques. Med Phys 2013;40:011714. https://doi.org/10.1118/1.4770285.

[27] Lowther NJ, Marsh SH, Louwe RJW. Dose accumulation to assess the validity of treatment plans with reduced margins in radiotherapy of head and neck cancer. Phys Imaging Radiat Oncol 2020;14:53–60. https://doi.org/10.1016/j.phro.2020.05.004.

[28] Kanda Y. Investigation of the freely available easy-to-use software "EZR" for medical statistics. Bone Marrow Transplant 2013;48:452–8. https://doi.org/10.1038/bmt.2012.244.

[29] Taasti VT, Hong L, Shim JSA, Deasy JO, Zarepisheh M. Automating proton treatment planning with beam angle selection using Bayesian optimization. Med Phys 2020;47:3286–96. https://doi.org/10.1002/mp.14215.

[30] Frazier PI. Bayesian optimization. In: Recent advances in optimization and modeling of contemporary problems. INFORMS; 2018, p. 255–78. https://doi.org/10.1287/educ.2018.0188.

[31] Spiegelhalter DJ, Abrams KR, Myles JP. Bayesian approaches to clinical trials and health-care evaluation, Vol. 13. John Wiley & Sons; 2004.

[32] Halpern JY. Reasoning about uncertainty. MIT Press; 2017.

[33] Xie Y, Wang Q, Hu T, Chen R, Wang J, Chang H, et al. Risk factors related to acute radiation dermatitis in breast cancer patients after radiotherapy: a systematic review and meta-analysis. Front Oncol 2021;11:738851. https://doi.org/10.3389/fonc.2021.738851.

[34] Chugh R, Bisht YS, Nautiyal V, Jindal R. Factors influencing the severity of acute radiation-induced skin and mucosal toxicity in head and neck cancer. Cureus 2021;13:e18147.

[35] Villavicencio M, Granados-García M, Vilajosana E, Domínguez-Cherit J. Management of radiodermatitis associated with cetuximab in squamous cell carcinomas of the head and neck. Int J Dermatol 2017;56:602–9. https://doi.org/10.1111/ijd.13507.

[36] Bölke E, Gerber PA, Lammering G, Peiper M, Müller-Homey A, Pape H, et al. Development and management of severe cutaneous side effects in head-and-neck cancer patients during concurrent radiotherapy and cetuximab. Strahlenther Onkol 2008;184:105–10. https://doi.org/10.1007/s00066-008-1829-z.

[37] Bonomo P, Loi M, Desideri I, Olmetto E, Delli Paoli CD, Terziani F, et al. Incidence of skin toxicity in squamous cell carcinoma of the head and neck treated with radiotherapy and cetuximab: a systematic review. Crit Rev Oncol Hematol 2017;120:98–110. https://doi.org/10.1016/j.critrevonc.2017.10.011.

[38] Budach W, Bölke E, Homey B. Severe cutaneous reaction during radiation therapy with concurrent cetuximab. N Engl J Med 2007;357:514–5. https://doi.org/10.1056/NEJMc071075.

[39] Merlano M, Russi E, Benasso M, Corvò R, Colantonio I, Vigna-Taglianti R, et al. Cisplatin-based chemoradiation plus cetuximab in locally advanced head and neck cancer: a phase II clinical study. Ann Oncol 2011;22:712–7. https://doi.org/10.1093/annonc/mdq412.

[40] Berger B, Belka C. Severe skin reaction secondary to concomitant radiotherapy plus cetuximab. Radiat Oncol 2008;3:5. https://doi.org/10.1186/1748-717X-3-5.

[41] Meyer F, Fortin A, Wang CS, Liu G, Bairati I. Predictors of severe acute and late toxicities in patients with localized head-and-neck cancer treated with radiation therapy. Int J Radiat Oncol Biol Phys 2012;82:1454–62. https://doi.org/10.1016/j.ijrobp.2011.04.022.

[42] de Aguiar BRL, Guerra ENS, dos Reis PED. Radiogenomics: a personalized strategy for predicting radiation-induced dermatitis 2022. https://doi.org/10.5772/intechopen.108745.

[43] Yu J, Huang Y, Liu L, Wang J, Yin J, Huang L, et al. Genetic polymorphisms of Wnt/β-catenin pathway genes are associated with the efficacy and toxicities of radiotherapy in patients with nasopharyngeal carcinoma. Oncotarget 2016;7:82528–37. https://doi.org/10.18632/oncotarget.12754.

[44] Borchiellini D, Etienne-Grimaldi MC, Bensadoun RJ, Benezery K, Dassonville O, Poissonnet G, et al. Candidate apoptotic and DNA repair gene approach confirms involvement of ERCC1, ERCC5, TP53 and MDM2 in radiation-induced toxicity in head and neck cancer. Oral Oncol 2017;67:70–6. https://doi.org/10.1016/j.oraloncology.2017.02.003.

[45] Yamazaki H, Yoshida K, Kobayashi K, Tsubokura T, Kodani N, Aibe N, et al. Assessment of radiation dermatitis using objective analysis for patients with breast cancer treated with breast-conserving therapy: influence of body weight. Jpn J Radiol 2012;30:486–91. https://doi.org/10.1007/s11604-012-0073-8.

[46] Palazzi M, Tomatis S, Orlandi E, Guzzo M, Sangalli C, Potepan P, et al. Effects of treatment intensification on acute local toxicity during radiotherapy for head and neck cancer: prospective observational study validating CTCAE. version 3.0, scoring system. Int J Radiat Oncol Biol Phys 2008;70:330–7. https://doi.org/10.1016/j.ijrobp.2007.06.022.

[47] McQuestion M. Evidence-based skin care management in radiation therapy: clinical update. In: Semin Oncol Nurs. W. B. Saunders 2011;27:e1–e17. https://doi.org/10.1016/j.soncn.2011.02.009.

[48] Park JH, Byun HJ, Lee JH, Kim H, Noh JM, Kim CR, et al. Feasibility of photobiomodulation therapy for the prevention of radiodermatitis: a single-institution pilot study. Lasers Med Sci 2020;35:1119–27. https://doi.org/10.1007/s10103-019-02930-1.

[49] Kuga MC, Tonetto MR, Caetano RD, Castro PH, Soares AC. Smoking influences the occurrence of radiodermatitis in head and neck-irradiated patients. World J Dent 2017;8:55–8. https://doi.org/10.5005/jp-journals-10015-1411.

[50] Bontempo PSM, Ciol MA, Menêses AGD, Simino GPR, Ferreira EB, Reis PEDD. Acute radiodermatitis in cancer patients: incidence and severity estimates. Rev Esc Enferm USP 2021;55:e03676.

[51] Cardozo ADS, Simões FV, Santos VO, Portela LF, Silva RCD. Severe radiodermatitis and risk factors associated in head and neck cancer patients. Texto contexto - enferm 2020;29. https://doi.org/10.1590/1980-265X-TCE-2018-0343.

[52] İnan GA, Arslan A, Aral İP, Arslan SA. Factors on development and severity of acute radiodermatitis: prospective single-centre study. Anatolian Curr Med J 2022;4:356–61. https://doi.org/10.21203/rs.3.rs-1456948/v1.

[53] Bibault JE, Dussart S, Pommier P, Morelle M, Huguet M, Boisselier P, et al. Clinical outcomes of several IMRT techniques for patients with head and neck cancer: a propensity score–weighted analysis. Int J Radiat Oncol Biol Phys 2017;99:929–37. https://doi.org/10.1016/j.ijrobp.2017.06.2456.

[54] Roland TF, Stathakis S, Ramer R, Papanikolaou N. Measurement and comparison of skin dose for prostate and head-and-neck patients treated on various IMRT delivery systems. Appl Radiat Isot 2008;66:1844–9. https://doi.org/10.1016/j.apradiso.2008.05.003.

[55] Capelle L, Warkentin H, MacKenzie M, Joseph K, Gabos Z, Pervez N, et al. Skin-sparing helical tomotherapy vs 3D-conformal radiotherapy for adjuvant breast radiotherapy: in vivo skin dosimetry study. e590 Int J Radiat Oncol Biol Phys 2012;83:e583. https://doi.org/10.1016/j.ijrobp.2012.01.086.

[56] Dias AG, Pinto DFS, Borges MF, Pereira MH, Santos JAM, Cunha LT, et al. Optimization of skin dose using in-vivo MOSFET dose measurements in bolus/non-bolus fraction ratio: a VMAT and a 3DCRT study. J Appl Clin Med Phys 2019;20:63–70. https://doi.org/10.1002/acm2.12525.

[57] Al-Shareef JM, Attalla EM, El-Gebaly RH, Deiab NA, Mokhtar MH, Fathy MM. Peripheral and surface dose assessment using diode and Gafchromic EBT3 films dosimeters for different radiotherapy techniques. Radiat Phys Chem 2022;198:110237. https://doi.org/10.1016/j.radphyschem.2022.110237.

[58] Dobler B, Obermeier T, Hautmann MG, Khemissi A, Koelbl O. Simultaneous integrated boost therapy of carcinoma of the hypopharynx/larynx with and without flattening filter – a treatment planning and dosimetry study. Radiat Oncol 2017;12:114. https://doi.org/10.1186/s13014-017-0850-8.

[59] Lee N, Chuang C, Quivey JM, Phillips TL, Akazawa P, Verhey LJ, et al. Skin toxicity due to intensity-modulated radiotherapy for head-and-neck carcinoma. Int J Radiat Oncol Biol Phys 2002;53:630–7. https://doi.org/10.1016/S0360-3016(02)02756-6.

[60] Radaideh K. Evaluation of thermoplastic Klarity mask use during intensity-modulated radiation therapy for head and neck carcinoma. J Radiother Pract 2018;17:171–8. https://doi.org/10.1017/S1460396917000632.

[61] Al-Mamgani A, van Rooij P, Verduijn GM, Mehilal R, Kerrebijn JD, Levendag PC. The impact of treatment modality and radiation technique on outcomes and toxicity of patients with locally advanced oropharyngeal cancer. Laryngoscope 2013;123:386–93. https://doi.org/10.1002/lary.23699.

[62] Bahl A, Oinam AS, Kaur S, Verma R, Elangovan A, Bhandari S, et al. Evaluation of acute toxicity and early clinical outcome in head and neck cancers treated with conventional radiotherapy and simultaneous integrated boost arc radiotherapy. World J Oncol 2017;8:117–21. https://doi.org/10.14740/wjon1049w.

[63] Penoncello GP, Ding GX. Skin dose differences between intensity-modulated radiation therapy and volumetric-modulated arc therapy and between boost and integrated treatment regimens for treating head and neck and other cancer sites in patients. Med Dosim 2016;41:80–6. https://doi.org/10.1016/j.meddos.2015.09.001.

[64] Soto LA, Casey KM, Wang J, Blaney A, Manjappa R, Breitkreutz D, et al. FLASH irradiation results in reduced severe skin toxicity compared to conventional-dose-rate irradiation. Radiat Res 2020;194:618–24. https://doi.org/10.1667/RADE-20-00090.

[65] Abel E, Girdhani S, Jackson I, Eley J, Katsis A, Marshall A, et al. Characterization of radiation-induced lung fibrosis and mode of cell death using single and multi-pulsed proton flash irradiation. E653 Int J Radiat Oncol Biol Phys 2019;105:E652. https://doi.org/10.1016/j.ijrobp.2019.06.1033.

[66] Avanzo M, Drigo A, Kaiser SR, Roggio A, Sartor G, Chiovati P, et al. Dose to the skin in helical tomotherapy: results of in vivo measurements with radiochromic films. Phys Med 2013;29:304–11. https://doi.org/10.1016/j.ejmp.2012.04.004.

[67] Higgins PD, Han EY, Yuan JL, Hui S, Lee CK. Evaluation of surface and superficial dose for head and neck treatments using conventional or intensity-modulated techniques. Phys Med Biol 2007;52:1135–46. https://doi.org/10.1088/0031-9155/52/4/018.

[68] Price Jr RA, Koren S, Veltchev I, Hossain M, Lin MH, Galloway T, et al. Planning target volume-to-skin proximity for head-and-neck intensity modulated radiation therapy treatment planning. e29 Pract Radiat Oncol 2014;4:e21. https://doi.org/10.1016/j.prro.2013.04.002.

[69] Srivastava SP, Cheng CW, Das IJ. The dosimetric and radiobiological impact of calculation grid size on head and neck IMRT. Pract Radiat Oncol 2017;7:209–17. https://doi.org/10.1016/j.prro.2016.10.001.
[70] Razali NM, Wah YB. Power comparisons of Shapiro-Wilk, Kolmogorov-Smirnov, Lilliefors and Anderson-Darling tests. J Stat Model Analyt 2011;2:21–33. https://www.researchgate.net/publication/267205556.
[71] Leventhal J, Young MR. Radiation dermatitis: recognition, prevention, and management. Oncology (Williston Park) 2017;31(885–7):894–9. https://europepmc.org/article/med/29297172.